ACS APPLIED MATERIALS & INTERFACES

Research Article

www.acsami.org

Highly Efficient Antibacterial Surface Grafted with a Triclosan-Decorated Poly(*N*-Hydroxyethylacrylamide) Brush

Hai-Xia Wu,[†,‡] Lei Tan,[†] Zhao-Wen Tang,[†] Mei-Yan Yang,[†] Jian-Yun Xiao,[†] Chuan-Jun Liu,*[,†] and Ren-Xi Zhuo[†]

[†]Key Laboratory of Biomedical Polymers of Ministry of Education, College of Chemistry and Molecular Science, Wuhan University, Wuhan, Hubei 430072, P. R. China

[‡]College of Chemistry and Chemical Engineering, Luoyang Normal University, Luoyang, Henan 471022, P. R. China

Supporting Information

ABSTRACT: This work presented a highly efficient antibacterial Ti-surface which was grafted with poly(*N*-hydroxyethylacrylamide) (PHEAA) brush and further decorated with triclosan (TCS). The modified surfaces were characterized using contact angle measurements, X-ray photoelectron spectroscopy, and attenuated total reflectance Fourier transform infrared. The antibacterial performance of the modified surfaces was evaluated using the *Streptococcus mutans* and *Actinomyces naeslundii* attachment test. The Ti surface with PHEAA brush (Ti-PHEAA) was able to resist the adhesion of the bacteria, while the TCS-decorated Ti surface (Ti-TCS) showed the capability of killing the bacteria adhered on the surface. As we coupled the TCS to the PHEAA brush, the surface showed highly efficient antibacterial performance due to the combination of the resistance to the bacteria adhesion and its activity of killing bacteria.

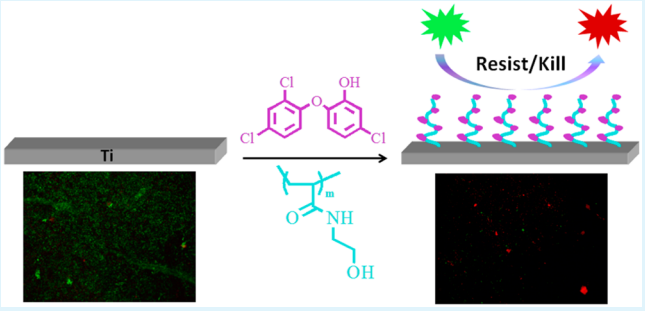

KEYWORDS: *antibacterial surface, poly(N-hydroxyethylacrylamide), surface grafting, triclosan, resistance to bacterial adhesion, polymer brush*

INTRODUCTION

The adhesion and proliferation of bacteria on a material's surface and the subsequent formation of biofilm create challenges in healthcare, such as surgical equipment in hospitals and medical implants.[1,2] For example, the implant-associated infections resulting from the adhesion of bacterial and subsequent biofilm formation are a major cause of morbidity and mortality.[3] Great efforts have been made to prevent the adhesion of bacteria and subsequent biofilm on a material's surface. Bacterial adhesion on the surface is a complex process determined by the nature of bacteria, the surrounding environment, and the property of the material's surface. The design and exploration of antibacterial materials have been a long-standing effort, and many strategies have been presented to prevent the bacteria colonization on the material's surface.

There are two strategies to design the efficient antibacterial surface: one is to realize the antibacterial capability by killing the bacteria adhered on the surface, and the other is to achieve the antibacterial effect through the resistance to adhesion of proteins and bacteria on the surface.[4−8] Teaching biocides to kill the adhered bacteria on the surface is the common method for the design of antibacterial materials. However, a major disadvantage of teaching biocides is that they subsequently end up in the environment, which would bring out adverse effects. Hence, it is suggested to be used prudently.[9,10] Moreover, ammonium cation polymers, such as poly(2-dimethylaminoethyl methacrylate) (DMAEMA)[11,12] and poly(4-vinylpyridine) (4VP),[13] have been widely used as antibacterial materials by leading to the death of contact bacteria. Metal ions, such as Ag^+ and Cu^{2+}, are popular antibacterial materials which cause the death of adhered bacteria. The materials will lose their antibacterial effect when the metal coating is dissolved completely from the surface.[14,15] Furthermore, the widespread use of metal as an antibacterial coating could release metal ions into the environment, which has potential implications for human health and the environment.[16,17] For the antibacterial surface, the accumulated dead bacteria on the surface would dramatically decrease its antibacterial efficiency in most cases.

It is crucial to develop environmental friendly and long-term antibacterial materials. Recently, the prevention of bacteria adhesion by the modified polymer layers has attracted attention increasingly. The polymers used as antibacterial coating mainly include hydrophilic polymers, zwitterions polymers, and superhydrophobic polymers and amphiphilic coating.[18−20] Among the hydrophilic polymer, the polyethylene glycol (PEG) systems are popularly used as antibacterial materi-

Received: February 7, 2015
Accepted: March 10, 2015
Published: March 10, 2015

DOI: 10.1021/acsami.5b01210
ACS Appl. Mater. Interfaces 2015, 7, 7008−7015

Scheme 1. Schematic Representation of the Ti Surface Grafted with a PHEAA Brush and Decorated with TCS

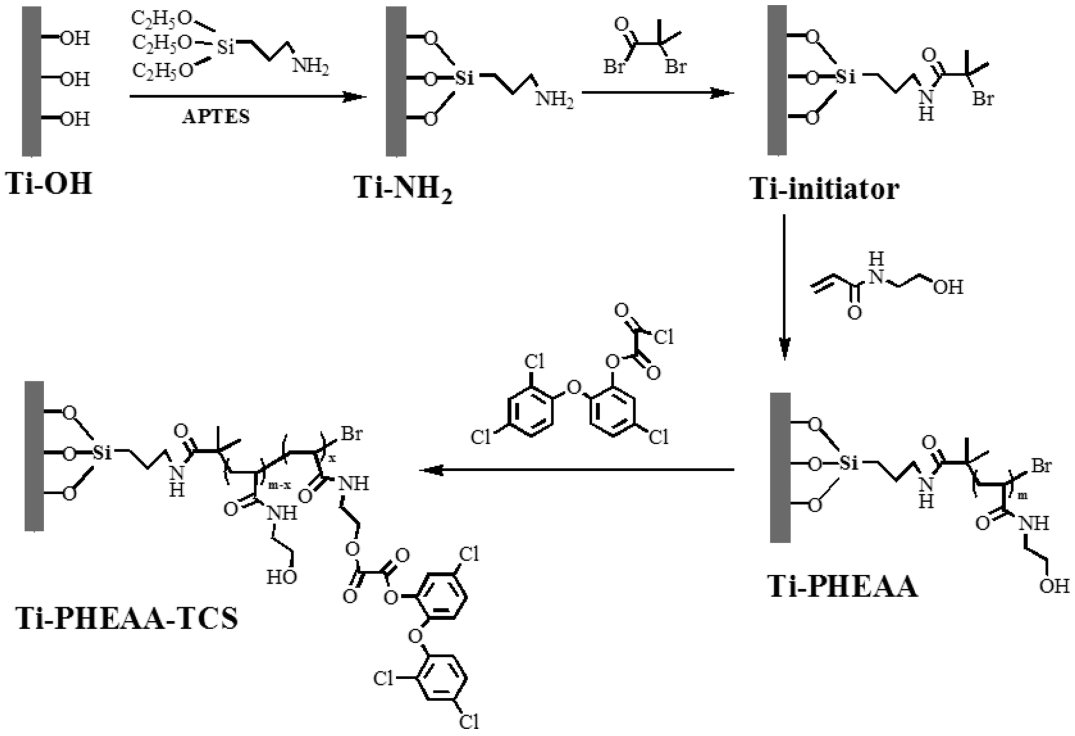

als.[21−23] Its antibacterial performance was attributed to the hydration layer created via hydrogen bonds to inhibit protein adsorption and bacterial adhesion. As an alternative, zwitterionic polymers showed effectively antiadhesion performance because of the formation of hydration constructed by the zwitterionic head.[24−28] The design of antibacterial materials based on superhydrophobic surfaces is another strategy. The superhydrophobic surfaces can significantly reduce the amount of adhered bacteria, which could be removed easily from the surfaces compared with that on hydrophilic or hydrophobic surfaces.[29,30] However, the efficiency would dramatically decrease with the extension of time due to the fully wetting and the entrapped air at the surface.[31,32]

A good strategy for the design of an antibacterial material would be to combine the substance with resistance to bacterial adhesion and antibacterial moieties to improve and prolong the antibacterial activity.[33−38] However, it is crucial to explore stable and long-term antibacterial materials with both the properties of repelling bacterial attachment and contact-killing bacteria. Poly(*N*-hydroxyethylacrylamide) (PHEAA) was an electrically neutral, biocompatible, thermo-tolerant polymer and exhibited effective resistance to proteins and bacteria adhesion attributing to the stronger association with interfacial water, which was reported by Zhao and Zheng.[39] While the simple polymer brush coating could not show complete prevention of bacterial adhesion, unfortunately, a small amount of adhering bacteria may form a mature biofilm and cause a fatal consequence. Triclosan (TCS) is a widely used broad-spectrum antibacterial agent with immediate and persistent antibacterial effectiveness.[40,41] In this paper, we report a highly efficient antibacterial Ti-surface with stable and potential long-term antibacterial performance, which was grafted with a poly(*N*-hydroxyethylacrylamide) (PHEAA) brush and further decorated with triclosan (TCS). The PHEAA brush on Ti surface was prepared using surface-initiated atomic transfer radical polymerization (SI-ATRP), and the TCS was covalently attached to the PHEAA brush. The antibacterial performance of the modified surfaces was evaluated using the *Streptococcus mutans* and *Actinomyces naeslundii* attachment test.

EXPERIMENTAL SECTION

Materials. Commercially pure grade 2 Ti discs with a diameter of 10 mm and thickness of 1 mm were purchased from Northwest Institute for Nonferrous Metal Research (Xi'an, China). 3-Aminopropyltriethoxysilane (APTES, 206.35 g/mol, 97%), bromoisobutyryl bromide (BIBB, 229.9 g/mol, 99%), and ethyl 2-bromoisobutyrate (EBIB, 195.05 g/mol, 98%) were purchased from Aladdin Chemistry Co. Ltd. *N*-Hydroxyethylacrylamide (HEAA, 115.13 g/mol, 98.0%) was supplied by TCI (Shanghai) Development Co., Ltd. Tris[2-(dimethylamino)ethyl]amine (Me_6TREN, 230.4 g/mol, 99%) was donated by Alfa. 5-[Chloro-2-(2,4-dichlorophenoxy)phenol] (Triclosan, TCS, 289.54 g/mol, 97.0%) was purchased from Shanghai Kayon Biological Technology Co., Ltd. Oxalylc chloride (126.93 g/mol, 98%) was supplied by Shanghai Chemical Reagent Co. All the reagents mentioned above were used as received. Copper(I) bromide (CuBr, 98.5%, Shanghai Chemical Reagent Co Ltd.) was purified by stirring in acetic acid, washing with acetone and ethanol, and then drying under vacuum. Triethylamine (TEA, 101.19 g/mol, 98%) and all other solvents were purchased from Shanghai Chemical Reagent Co. Ltd. and purified according to standard methods. Deionized water purified by a Millipore water purification system to give a minimum resistivity of 18.2 MΩ·cm was used in all experiments. Argon gas was of high-purity grade.

Preparation of Antibacterial Surfaces. The procedure of preparing the antibacterial Ti surfaces is shown in Scheme 1. Prior to the surface modification, Ti discs were polished with a series of SiC abrasive papers of 360, 600, 1000, 1500, 2000, 2500, and 3000.[42] The polished Ti discs were cleaned ultrasonically for 10 min in DI water, sodium hydroxide aqueous (5.0 wt %), acetone, petroleum ether, isopropyl alcohol, and DI water in that order. Then, the discs were dried at room temperature to obtain Ti−OH substrates.[3]

The freshly prepared Ti−OH discs were immersed in the toluene solution of 3-aminopropyltriethoxysilane (APTES, 2.5 vol %) at room

DOI: 10.1021/acsami.5b01210
ACS Appl. Mater. Interfaces 2015, 7, 7008−7015

temperature overnight to obtain Ti-NH_2. Afterward, the Ti discs were ultrasonically washed successively with toluene, dichloromethane, ethanol, and DI water. After the discs were dried in an argon stream, the prepared Ti-NH_2 disc was soaked in a solution of TEA (0.1 mL, 0.7 mmol) in dry dichloromethane (20 mL). Then, BIBB (0.5 mL, 4.04 mmol) was added dropwise into the solution, and the reaction was performed at 0 °C for 2 h and kept at room temperature overnight. The modified Ti discs were taken out and ultrasonically washed successively with toluene; dichloromethane, ethanol, and DI water and then dried in an argon stream to obtain the Ti-initiator surface.[43] Subsequently, the PHEAA brush was grafted from the Ti-initiator surface by SI-ATRP. Typically, a mixture of Ti-initiator disc, HEAA monomers (1 g, 8.69 mmol), Me_6TREN (40 mg, 0.174 mmol), initiator EBIB (25 μL, 0.172 mmol), and 1:1 ethanol/water (4 mL) was placed in a glass tube. The mixture was deoxygenated by four freeze-pump-fill argon-thaw cycles, and during the second cycle, CuBr (25 mg, 0.174 mmol) was added to the tube under the protection of argon. The polymerization was kept stirring in the oil bath at 29 °C for 72 h and then stopped by exposure to air. The grafted Ti discs with PHEAA were ultrasonically washed repeatedly two times with water and then dried in an argon stream to obtain the Ti surface with a PHEAA brush (Ti-PHEAA) disc.[44,45]

The solution of TCS (2.9 g, 10 mmol) in dry dichloromethane (10 mL) containing TEA (2.09 mL, 5 mmol) was added dropwise into the solution of oxalylc chloride (1.28 mL, 15 mmol) in anhydrous dichloromethane (5 mL) with stirring under the protection of argon at 0 °C for 2 h. Then, the reaction was maintained for 2 h at room temperature. After the reaction, the solvent and the unreacted oxalylc chloride were removed from the mixture by vacuum rotary evaporation to obtain the product. The Ti-PHEAA or Ti-NH_2 disc was added to the solution of product in anhydrous dichloromethane under the protection of argon with stirring, and the reaction was kept at room temperature overnight. Afterward, the modified Ti disc was taken out from solution and was ultrasonically cleaned with dichloromethane, ethanol, and ID water, successively, and dried in an argon stream to obtain the Ti-PHEAA-TCS or TCS-decorated Ti surface (Ti-TCS).

Characterization of the Modified Ti Surfaces. The static water contact angle (WCA) on the modified Ti surface was measured by the sessile drop method using the contact angle measuring system (OCA20, Dataphysics Instruments with GmbH, Germany). The measurements were performed using 2 μL of a DI water droplet at ambient temperature. The value reported is the average of three measurements taken from different locations of the surface.

The surface composition of the modified Ti discs was characterized by X-ray photoelectron spectroscopy (XPS) (KRATOS XSAM800) using Mg K (1253.6 eV) as the radiation source. The spectra were collected at photoelectron take off angles of 90° with respect to the sample surface, and the binding energy (BE) scale is calibrated by C 1s of the hydrocarbon peak at 284.8 eV. Survey spectra were run in the binding energy range of 0−800 eV, and the spectra of Br 3d, C 1s, N 1s, O 1s, and Cl 2p were collected. In addition, a high-resolution C 1s spectrum was fitted using a Shirley background subtraction and a series of Gaussian peaks.

Attenuated total reflectance Fourier transform infrared (ATR-FTIR) spectra were used to verify that the Ti-PHEAA-TCS was achieved successfully, and the details of the ATR-FTIR measurement were shown in the Supporting Information. The morphology of the modified Ti surface and the PHEAA brush was characterized using an atomic force microscope (AFM).

Bacterial Attachment. *Streptococcus mutans* (*S. muntans*, ATCC35668) and *Actinomyces naeslundii* (ATCC35668) were adopted to investigate the antibacterial performance of the as-modified Ti discs. Each kind of bacteria was cultured in a medium containing 15.0 mg/mL tryptone, 5.0 mg/mL soytone, and 15 mg/mL NaCl under anaerobic conditions at 37 °C for 24 h. After examining the morphology, the single colonies scraped from tablets were cultured by continuously passaging until the third generation in the medium of BHI (brain heart infusion, 10 mL) under anaerobic conditions at 37 °C for 16 h. When the OD value of *S. muntans* reached 0.30 and that of *Actinomyces naeslundii* reached 0.50, the bacteria were used in the attachment assay.

After 1 h of ultraviolet irradiation, the prepared Ti discs were placed in a 24-well plate, and then 10 μL of bacteria suspension and 1 mL of BHI medium containing 1% sugar were added to each well in that order. Bacteria were incubated with the samples in an incubator for 4 or 24 h at 37 °C, and then, the bacterial solution was removed. The Ti discs were washed with phosphate buffered saline (PBS, pH = 7.4) 3 times for SEM and fluorescent microscope (FM) imaging. Prior to being observed using SEM (FEI QUANTA 200), the Ti discs with bacteria were placed in glutaraldehyde (2.5 wt %) solution for 2 h, followed by dehydration with graded ethanol solutions of 50%, 60%, 70%, 80%, 90%, and 100% and then dried. The SEM images were taken on the surface after Au sputtering.

The fluorescent microscope (FM, Leica Dm4000B Germany) was also used to evaluate the amount of adhered bacteria on the Ti discs. Bacteria adhering to sample surfaces were subsequently stained with 1 mL of a Live/Dead Bacterial Viability Kit for 15 min in a dark room at ambient temperature based on the principle in previous literature.[46] The Ti discs with stained bacteria were observed by a FM with 50× magnification, and the images were taken at λ_{ex} = 488 nm/λ_{em}= 520 nm for detection with a Live/Dead Bacterial Viability Kit, which were analyzed by Image Plus software.

RESULTS AND DISCUSSION

Characterization of the Modified Ti Surfaces. The WCA of the Ti surface modified in different steps was displayed in Figure 1, which provided the information on the surface

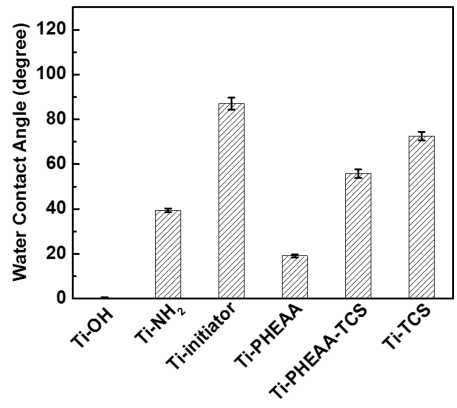

Figure 1. Contact angle measurement of the modified Ti surfaces.

wettability. The WCA on the hydrophilic Ti−OH surface is close to zero degrees, and it increased to 40° after the introduction of APTES, suggesting APTES was successfully anchored on the Ti−OH surface. After the immobilization of initiator BIBB, the WCA increased to 87°, indicating that the initiator was successfully immobilized on the Ti-NH_2 surface. The WCA decreased to 19° after the grafting of the hydrophilic PHEAA brush onto the Ti-initiator surface. The WCA on Ti-PHEAA-TCS increased to 56°, and the increase of hydrophobicity was attributed to the successful decoration of TCS to the Ti-PHEAA surface. Similarly, when the Ti-NH_2 surface was decorated by TCS, the WCA increased to 73°.

To confirm the achievement of multistep-modified surfaces, XPS was employed to measure the surface chemistry composition. The XPS spectra of modified Ti surfaces and atomic compositions are shown in Figure 2 and Table 1. Compared with the XPS spectra of the Ti-NH_2 surface, there was a new peak at 69 eV assigned to Br 3d (the enlarged feature of Figure 2 was shown in Figure S1 in the Supporting Information) in the spectra of the Ti-initiator surface. This

DOI: 10.1021/acsami.5b01210
ACS Appl. Mater. Interfaces 2015, 7, 7008−7015

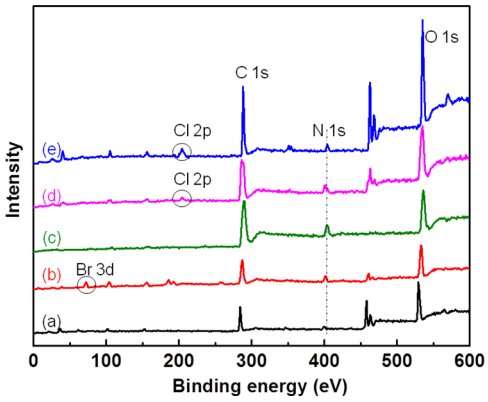

Figure 2. XPS survey spectra of the (a) Ti-NH_2, (b) Ti-initiator, (c) Ti-PHEAA, (d) Ti-PHEAA-TCS, and (e) Ti-TCS surface.

Table 1. Elemental Composition of Ti-NH_2, Ti-Initiator, Ti-PHEAA, Ti-PHEAA-TCS, and Ti-TCS Surface Determined by XPS Analysis

	XPS atomic concentration (at %)				
samples	C	O	N	Br	Cl
Ti-NH_2	53.1	41.3	5.6		
Ti-initiator	61.2	27.6	7.1	4.1	
Ti-PHEAA	62.9	25.7	10.9	0.5	
Ti-PHEAA-TCS	66.1	24.4	6.2		3.3
Ti-TCS	52.5	35.2	4.2		8.1

information confirmed that the initiator was successfully immobilized on the surface. After grafting the PHEAA brush on the surface, the intensity of the N 1s signal increased, and the relative content of N increased to 10.9 (at %) from 7.1 (at %), as shown in Table 1. The atomic ratio of C/O/N was 62.9/25.7/10.9 from XPS spectra, which is consistent with the calculated value 5/2/1 based on the molecular formula. In the high-resolution C 1s spectra of Ti-PHEAA (as shown in Figure S2, Supporting Information), C═O around 288.5 eV was mainly attributed to amide carbon O═C−N in PHEAA. This is reasonable since the ratio of C−O (N, Br)/C═O is 50.3/25.3, which is almost equally to the value 2/1 in the molecular formula of HEAA. These results confirmed the successful grafting of PHEAA on the Ti-initiator surface. In the XPS spectra of Ti-PHEAA-TCS and Ti-TCS, a new signal at 204 eV appeared, which was attributed to Cl 2p from TCS and indicated the successful decoration of TCS on the surface. The grafting ratio of TCS on PHEAA was estimated to be 16% according to the atomic concentration of N and Cl in Table 1.

ATR-FTIR was used to monitor the modification in different processes. The infrared spectra of modified Ti discs in different steps were displayed in Figure S3, Supporting Information. After the grafting of PHEAA on the surface, a broad peak appeared around 3300 cm^{-1} ascribed to −OH stretching vibration in PHEAA,[45,47] and the intensity of the peak at 1648 cm^{-1} assigned to the stretching vibration of C═O in amide increased remarkably. These results verified that the PHEAA brush was successfully grafted on the Ti-initiator surface.

Antibacterial Assay. Gram-positive bacteria species, *S. muntans* and *Actinomyces naeslundii*, were used to assess the bacterial attachment on the modified Ti surface. The antibacterial effect of the modified Ti surface was illustrated through the comparison of the amount and viability of bacteria adhered on the surface after a 4 or 24 h incubation. The total amount of adhered bacteria was evaluated using SEM, as shown in Figures 3 and 4. A number of bacteria were observed on the bare Ti and the Ti-TCS surfaces for both *S. mutans* and *Actinomyces naeslundii*. Compared with the bare Ti and the Ti-TCS surfaces, there were much less bacteria on the Ti-PHEAA surface. Only a small amount of the bacteria appeared on the Ti-PHEAA-TCS surface, which demonstrated the efficient antibacterial capability of Ti-PHEAA-TCS.

The bacteria attached on the substrate surfaces included the viable and the dead bacteria. The live bacteria appeared in green and the dead appeared in red in the FM images after the sample was stained with the Live/Dead Bacterial Viability Kit. The representative live/dead FM images of the samples incubated for 4 h are shown in Figure 5, and the corresponding quantitative analysis is given in Figure 6. Similarly, the results of the antibacterial assay are shown in Figures 7 and 8 after the samples were incubated for 24 h.

In Figure 5, numerous *S. mutans* and *Actinomyces naeslundii*, stained primarily green with only a few single red colonies, were observed on the bare Ti surface, indicating that the viable bacteria of *S. mutans* and *Actinomyces naeslundii* were prone to attach on the bare Ti surface. The dead bacteria were mainly due to natural apoptosis during the bacteria growth process.[13,48]

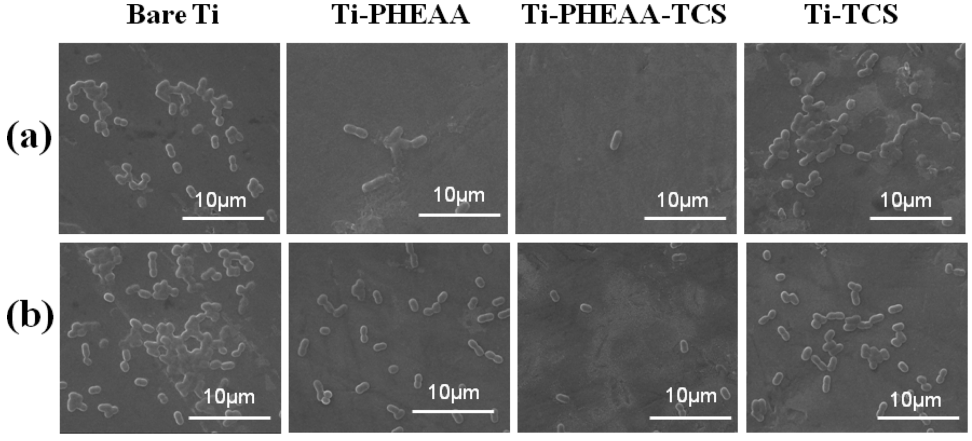

Figure 3. SEM images of the amount of (a) *S. mutans* and (b) *Actinomyces naeslundii* adhered after a 4 h incubation on the bare Ti, Ti-PHEAA, Ti-PHEAA-TCS, and Ti-TCS surface.

DOI: 10.1021/acsami.5b01210
ACS Appl. Mater. Interfaces 2015, 7, 7008−7015

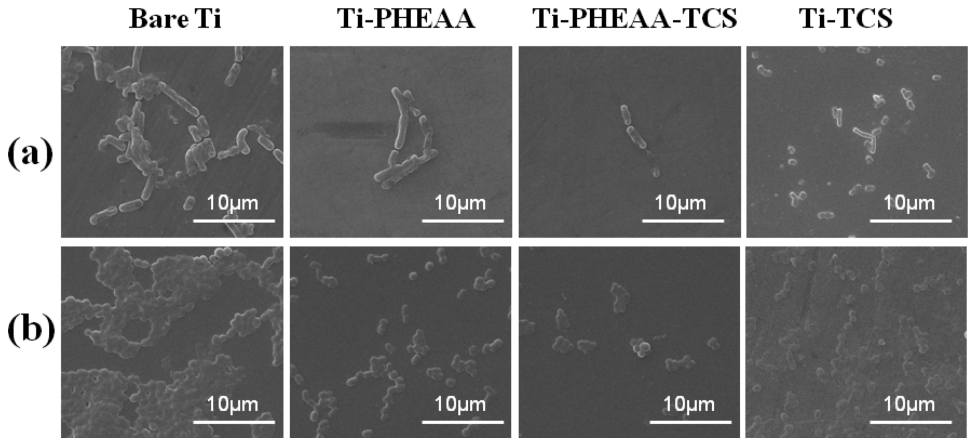

Figure 4. SEM images of the amount of (a) *S. mutans* and (b) *Actinomyces naeslundii* adhered after a 24 h incubation on the bare Ti, Ti-PHEAA, Ti-PHEAA-TCS, and Ti-TCS surface.

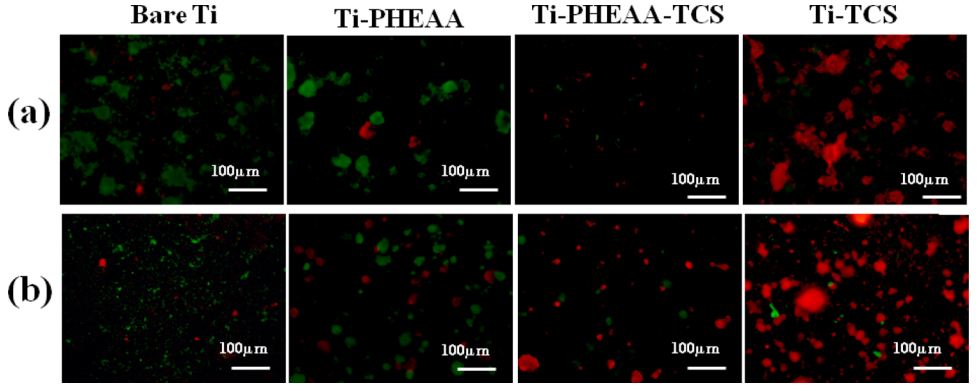

Figure 5. Representative fluorescence microscopy images of bare Ti, Ti-PHEAA, Ti-PHEAA-TCS, and Ti-TCS surfaces by live/dead bacteria staining after a 4 h incubation with (a) *S. mutans* and (b) *Actinomyces naeslundii*.

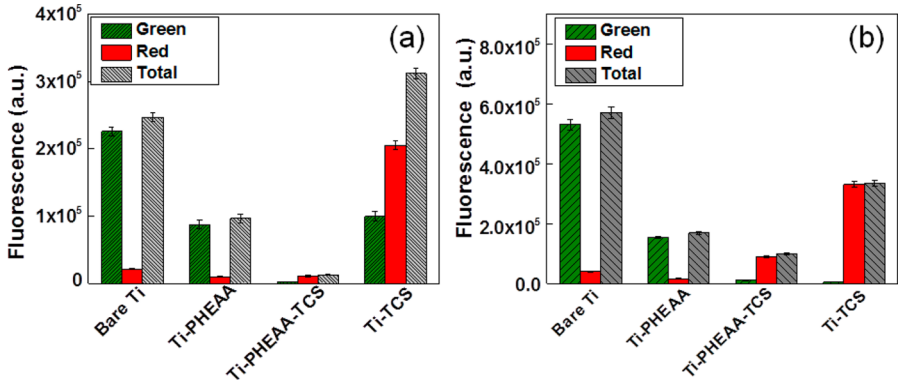

Figure 6. Quantitative analysis of (a) *S. mutans* and (b) *Actinomyces naeslundii* adhered on the bare Ti, Ti-PHEAA, Ti-PHEAA-TCS, and Ti-TCS surfaces after a 4 h incubation. The data were obtained on the basis of the FM images, and they are mean ± standard error, $n = 3$.

In the case of the Ti-TCS surface, there were a great number of bacteria, of which the minority were viable and majority were dead. This result demonstrated that the TCS bonded to the Ti surface exhibited a strong capability of killing bacteria. It was reported that the TCS forms a stable ternary complex by interacting with amino acid residues of the enzyme active site to affect the membrane structure and the function of the bacteria.[49,50] On the other hand, TCS bonded to the Ti surface still possesses effective antibacterial activity because the C−Cl bond was not destroyed during the aforementioned surface modification, while the body of dead bacteria would accumulate on the Ti-TCS surface with time due to the hydrophobicity of the surface.

It was generally considered that the hydrophilic surface possessed effective resistance to protein and bacteria,[39,47] which was also verified in this work. On the Ti-PHEAA surface, the amount of adherent bacteria was significantly reduced compared with that on the bare Ti surface. As shown in Figure 6, the amount of *S. mutans* on the Ti-PHEAA surface decreased by 60% and that of *Actinomyces naeslundii* was reduced by 68%. The ratio of green/red fluorescence was 9/1 for the two kinds of bacteria, which suggests the approximate

DOI: 10.1021/acsami.5b01210
ACS Appl. Mater. Interfaces 2015, 7, 7008−7015

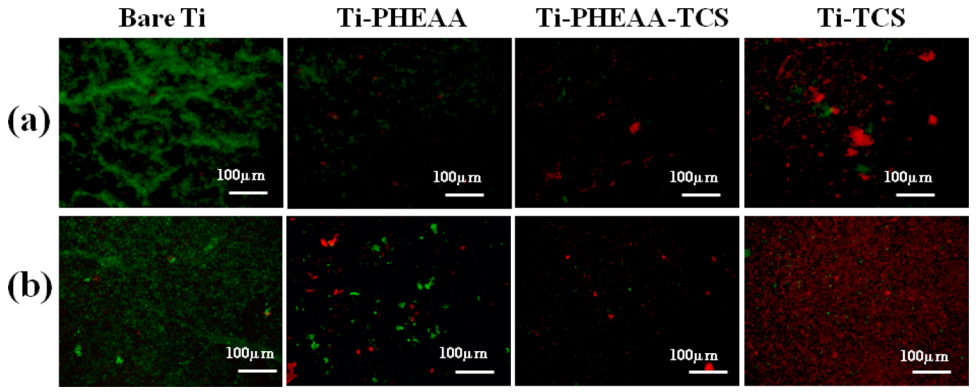

Figure 7. Representative fluorescence microscopy images of bare Ti, Ti-PHEAA, Ti-PHEAA-TCS, and Ti-TCS surfaces by live/dead bacteria staining after a 24 h incubation with (a) *S. mutans* and (b) *Actinomyces naeslundii*.

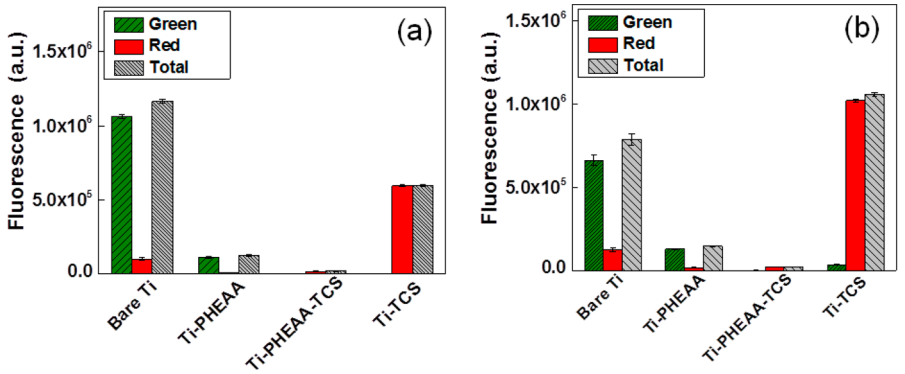

Figure 8. Quantitative analysis of (a) *S. mutans* and (b) *Actinomyces naeslundii* adhered on the bare Ti, Ti-PHEAA, Ti-PHEAA-TCS, and Ti-TCS surfaces after a 24 h incubation. The data were obtained on the basis of the FM images, and they are mean ± standard error, $n = 3$.

ratio of live/dead bacteria. It implied that the PHEAA brush could resist bacteria adhesion to some extent, which was in agreement with the results in previous literature.[45,51] It was considered that the highly hydrated PHEAA on the surface presents a large exclusion volume effect which inhibits protein and bacteria adhesion.[52−54]

In the case of the Ti-PHEAA-TCS surface, the amount of *S. mutans* and *Actinomyces naeslundii* adhered on the surface was reduced by 94% and 85%, respectively, compared with that on the bare Ti. The ratio of green/red fluorescence was 1/5 and 1/10 for *S. mutans* and *Actinomyces naeslundii*, which suggests the approximate ratio of live/dead bacteria. These analyses demonstrated that the Ti-PHEAA-TCS surface exhibited a highly efficient antibacterial capability attributed to the combination of resistance to bacterial adhesion and antibacterial agent.

To investigate the lasting antibacterial capability of the modified Ti surface, the results of the antibacterial assay after the samples incubated for 24 h are shown in Figures 7 and 8. There were a great number of live bacteria and a small number of dead bacteria on the bare Ti surface, while a small number of live bacteria and a great number of dead ones were bestrewed on the Ti-TCS surface. Compared with the bare Ti surface, the amount of *S. mutans* and *Actinomyces naeslundii* attaching on the Ti-PHEAA surface dramatically decreased, 89% and 82%, respectively. The ratio of green/red fluorescence was 10/1 for *S. mutans* and 8/1 for *Actinomyces naeslundii*. In the case of Ti-PHEAA-TCS, the amount of bacteria adhered on the surface reduced by 97% for both *S. mutans* and *Actinomyces naeslundii*. The ratio of live/dead was about 1/8 and 1/11 for *S. mutans* and *Actinomyces naeslundii* from the ratio of green/red fluorescence.

The antibacterial performance of the bare Ti, Ti-TCS, Ti-PHEAA, and Ti-PHEAA-TCS surface showed a similar trend in Figures 5 and 7. After a 4 and 24 h incubation, there is no clear difference in the amount of bacteria on Ti-PHEAA, which indicates that the Ti-PHEAA surface kept its effective resistance to bacterial adhesion after a 24 h exposure to the bacteria. When the results from the 4 and 24 h incubation were compared, the amount of dead bacteria on the Ti-TCS surface increased dramatically. However, in the case of the Ti-PHEAA-TCS surface, there is no observable increase for both the live and dead bacteria. These results confirmed that the highly efficient antibacterial capability of the Ti-PHEAA-TCS surface did not weaken with the longer exposure to bacteria. This property could be attributed to the covalent attachment of TCS to the PHEAA brush.

CONCLUSIONS

In this work, we presented a highly efficient antibacterial Ti-PHEAA-TCS surface which was grafted with a poly(*N*-hydroxyethylacrylamide) (PHEAA) brush and further decorated with triclosan (TCS). The PHEAA brush was prepared by SI-ATRP, and the TCS was covalently tethered to the brush. The modified surfaces were characterized using WCA, XPS, and ATR-FTIR. The antibacterial performance of the modified surfaces was evaluated through a bacteria attachment assay, in which *Streptococcus mutans* and *Actinomyces naeslundii* were used. The Ti-PHEAA surface was able to resist the bacterial adhesion, while the Ti-TCS showed its activity of leading to

DOI: 10.1021/acsami.5b01210
ACS Appl. Mater. Interfaces 2015, 7, 7008−7015

death of the bacteria adhered on the surface. The Ti-PHEAA-TCS exhibited a highly efficient antibacterial capability resulting from the combination of the resistance of the PHEAA brush to bacterial adhesion and the antibacterial capability of TCS. After a 4 and 24 h incubation, the antibacterial capability of the Ti-PHEAA-TCS surface did not exhibit an observable reduction, indicating the highly efficient antibacterial capability had promise to be long-lasting. Therefore, as an environmentally friendly antibacterial material, Ti-PHEAA-TCS, with high efficiency and potentially long-term antibacterial properties, would be a good candidate in biomaterials and biotechnological applications, especially in dental implants.

■ ASSOCIATED CONTENT

Supporting Information

The experimental details of XPS, ATR-FTIR, and AFM; the magnified XPS spectra and the chemical group compositions in high-resolution C 1s spectra of the modified Ti surfaces; the ATR-FTIR spectra of the samples; the morphology of the modified surfaces and the thickness of polymer brushes, which were measured by AFM. This material is available free of charge via the Internet at http://pubs.acs.org.

■ AUTHOR INFORMATION

Corresponding Author

*E-mail: cjliu@whu.edu.cn.

Notes

The authors declare no competing financial interest.

■ ACKNOWLEDGMENTS

This research was financially supported by National Natural Science Foundation of China (21204070), the National Key Basic Research Program of China (2011CB606202), and the Natural Science Foundation of Hubei Province (2011CDB460).

■ REFERENCES

(1) Zhang, X.; Wang, L.; Levänen, E. Superhydrophobic Surfaces for the Reduction of Bacterial Adhesion. *RSC Adv.* **2013**, *3*, 12003−12020.
(2) Banerjee, I.; Pangule, R. C.; Kane, R. S. Antifouling Coatings: Recent Developments in the Design of Surfaces That Prevent Fouling by Proteins, Bacteria, and Marine Organisms. *Adv. Mater.* **2011**, *23*, 690−718.
(3) He, S.; Zhou, P.; Wang, L.; Xiong, X.; Zhang, Y.; Deng, Y.; Wei, S. Antibiotic-Decorated Titanium with Enhanced Antibacterial Activity through Adhesive Polydopamine for Dental/Bone Implant. *J. R. Soc. Interface* **2014**, *11*, 20140169.1−20140169.13.
(4) Hadjesfandiari, N.; Yu, K.; Mei, Y.; Kizhakkedathu, J. N. Polymer Brush-Based Approaches for the Development of Infection-Resistant Surfaces. *J. Mater. Chem. B* **2014**, *2*, 4968−4978.
(5) Wilke, P.; Börner, H. G. Mussel-Glue Derived Peptide−Polymer Conjugates to Realize Enzyme-Activated Antifouling Coatings. *ACS Macro Lett.* **2012**, *1*, 871−875.
(6) Sundaram, H.; Han, X.; Nowinski, A.; Ella-Menye, J.; Wimbish, C.; Marek, P.; Senecal, K.; Jiang, S. One-Step Dip Coating of Zwitterionic Sulfobetaine Polymers on Hydrophobic and Hydrophilic Surfaces. *ACS Appl. Mater. Interfaces* **2014**, *6*, 6664−6671.
(7) Xu, L.; Ma, P.; Yuan, B.; Chen, Q.; Lin, S.; Chen, X.; Hua, Z.; Shen, J. Anti-Biofouling Contact Lenses Bearing Surface-Immobilized Layers of Zwitterionic Polymer by One-Step Modification. *RSC Adv.* **2014**, *4*, 15030−15035.
(8) Chen, Z.; He, S.; Butt, H. J.; Wu, S. Photon Upconversion Lithography: Patterning of Biomaterials Using Near-Infrared Light. *Adv. Mater.* **2015**, DOI: 10.1002/adma.201405933.
(9) Lichter, J. A.; Van Vliet, K. J.; Rubner, M. F. Design of Antibacterial Surfaces and Interfaces: Polyelectrolyte Multilayers as a Multifunctional Platform. *Macromolecules* **2009**, *42*, 8573−8586.
(10) Neoh, K. G.; Kang, E. T. Combating Bacterial Colonization on Metals via Polymer Coatings: Relevance to Marine and Medical Applications. *ACS Appl. Mater. Interfaces* **2011**, *3*, 2808−2819.
(11) Fan, X.; Lin, L.; Dalsin, J.; Messersmith, P. Biomimetic Anchor for Surface-Initiated Polymerization from Metal Substrates. *J. Am. Chem. Soc.* **2005**, *127*, 15843−15847.
(12) Yuan, S. J.; Pehkonen, S. O.; Ting, Y. P.; Neoh, K. G.; Kang, E. T. Antibacterial Inorganic-Organic Hybrid Coatings on Stainless Steel via Consecutive Surface-Initiated Atom Transfer Radical Polymerization for Biocorrosion Prevention. *Langmuir* **2010**, *26*, 6728−6736.
(13) Yuan, S. J.; Pehkonen, S. O.; Ting, Y. P.; Neoh, K. G.; Kang, E. T. Inorganic-Organic Hybrid Coatings on Stainless Steel by Layer-by-Layer Deposition and Durface-Initiated Atom-Transfer-Radical Polymerization for Combating Biocorrosion. *ACS Appl. Mater. Interfaces* **2009**, *1*, 640−652.
(14) Rai, M.; Yadav, A.; Gade, A. Silver Nanoparticles as a New Generation of Antimicrobials. *Biotechnol. Adv.* **2009**, *27*, 76−83.
(15) Puniredd, S. R.; Jańczewski, D.; Go, D. P.; Zhu, X.; Guo, S.; Ming Teo, S. L.; Chen Lee, S. S.; Vancso, G. J. Imprinting of Metal Receptors into Multilayer Polyelectrolyte Films: Fabrication and Applications in Marine Antifouling. *Chem. Sci.* **2015**, *6*, 372−383.
(16) Marambio-Jones, C.; Hoek, E. M. V. A Review of the Antibacterial Effects of Silver Nanomaterials and Potential Implications for Human Health and the Environment. *J. Nanopart. Res.* **2010**, *12*, 1531−1551.
(17) Amit, G. S.; Simon, S. Molecular Genetics: Silver as a Biocide: Will Resistance Become a Problem? *Nat. Biotechnol.* **1998**, *16*, 888−888.
(18) Lowe, S.; O'Brien-Simpson, N. M.; Connal, L. A. Antibiofouling Polymer Interfaces: Poly(ethylene glycol) and Other Promising Candidates. *Polym. Chem.* **2015**, *6*, 198−212.
(19) Goli, K. K.; Rojas, O. J.; Genzer, J. Formation and Antifouling Properties of Amphiphilic Coatings on Polypropylene Fibers. *Biomacromolecules* **2012**, *13*, 3769−3779.
(20) Wang, X.; Berger, R.; Ramos, J. I.; Wang, T.; Koynov, K.; Liu, G.; Butt, H.-J.; Wu, S. Nanopatterns of Polymer Brushes for Understanding Protein Adsorption on the Nanoscale. *RSC Adv.* **2014**, *4*, 45059−45064.
(21) Sun, C.; Miao, J.; Yan, J.; Yang, K.; Mao, C.; Ju, J.; Shen, J. Applications of Antibiofouling PEG-Coating in Electrochemical Biosensors for Determination of Glucose in Whole Blood. *Electrochim. Acta* **2013**, *89*, 549−554.
(22) Chen, H.; Wang, L.; Yeh, J.; Wu, X.; Cao, Z.; Wang, Y. A.; Zhang, M.; Yang, L.; Mao, H. Reducing Non-Specific Binding and Uptake of Nanoparticles and Improving Cell Targeting with an Antifouling PEO-*b*-PγMPS Copolymer Coating. *Biomaterials* **2010**, *31*, 5397−5407.
(23) Eshet, I.; Freger, V.; Kasher, R.; Herzberg, M.; Lei, J.; Ulbricht, M. Chemical and Physical Factors in Design of Antibiofouling Polymer Coatings. *Biomacromolecules* **2011**, *12*, 2681−2685.
(24) Yang, R.; Xu, J.; Ozaydin-Ince, G.; Wong, S. Y.; Gleason, K. K. Surface-Tethered Zwitterionic Ultrathin Antifouling Coatings on Reverse Osmosis Membranes by Initiated Chemical Vapor Deposition. *Chem. Mater.* **2011**, *23*, 1263−1272.
(25) Chang, Y.; Liao, S.; Higuchi, A.; Ruaan, R.; Chu, C.; Chen, W. A Highly Stable Nonbiofouling Surface with Well-Packed Grafted Zwitterionic Polysulfobetaine for Plasma Protein Repulsion. *Langmuir* **2008**, *24*, 5453−5458.
(26) Liu, Q.; Singh, A.; Liu, L. Amino Acid-Based Zwitterionic Poly(serine methacrylate) as an Antifouling Material. *Biomacromolecules* **2013**, *14*, 226−231.
(27) Mi, L.; Jiang, S. Integrated Antimicrobial and Nonfouling Zwitterionic Polymers. *Angew. Chem., Int. Ed.* **2014**, *53*, 1746−1754.
(28) Yu, B.; Zheng, J.; Chang, Y.; Sin, M.; Chang, C.; Higuchi, A.; Sun, Y. Surface Zwitterionization of Titanium for a General Bio-Inert

DOI: 10.1021/acsami.5b01210
ACS Appl. Mater. Interfaces 2015, 7, 7008−7015

Control of Plasma Proteins, Blood Cells, Tissue Cells, and Bacteria. *Langmuir* **2014**, *30*, 7502−7512.
(29) Privett, B.; Youn, J.; Hong, S.; Lee, J.; Han, J.; Shin, J.; Schoenfisch, M. Antibacterial Fluorinated Silica Colloid Superhydrophobic Surfaces. *Langmuir* **2011**, *27*, 9597−9601.
(30) Fadeeva, E.; Truong, V. K.; Stiesch, M.; Chichkov, B. N.; Crawford, R. J.; Wang, J.; Ivanova, E. P. Bacterial Retention on Superhydrophobic Titanium Surfaces Fabricated by Femtosecond Laser Ablation. *Langmuir* **2011**, *27*, 3012−3019.
(31) Zhang, H.; Lamb, R.; Lewis, J. Engineering Nanoscale Roughness on Hydrophobic Surface—Preliminary Assessment of Fouling Behaviour. *Sci. Technol. Adv. Mater.* **2005**, *6*, 236−239.
(32) Mahalakshmi, P.; Vanithakumari, S.; Gopal, J.; Mudali, K.; Ra, J. B. Enhancing Corrosion and Biofouling Resistance through Superhydrophobic Surface Modification. *Curr. Sci.* **2011**, *101*, 1328−1336.
(33) Asadinezhad, A.; Novák, I.; Lehocký, M.; Sedlařík, V.; Vesel, A.; Junkar, I.; Sáha, P.; Chodák, I. A Physicochemical Approach to Render Antibacterial Surfaces on Plasma-Treated Medical-Grade PVC: Irgasan Coating. *Plasma Processes Polym.* **2010**, *7*, 504−514.
(34) Glinel, J.; Jonas, A.; Jouenne, T.; Leprince, J.; Galas, L.; W, A. H. Antibacterial and Antifouling Polymer Brushes Incorporating Antimicrobial Peptide. *Bioconjugate Chem.* **2009**, *20*, 71−77.
(35) Yang, C.; Ding, X.; Ono, R. J.; Lee, H.; Hsu, L. Y.; Tong, Y. W.; Hedrick, J.; Yang, Y. Y. Brush-Like Polycarbonates Containing Dopamine, Cations, and PEG Providing a Broad-Spectrum, Antibacterial, and Antifouling Surface via One-Step Coating. *Adv. Mater.* **2014**, *26*, 7346−7351.
(36) Hu, R.; Li, G.; Jiang, Y.; Zhang, Y.; Zou, J. J.; Wang, L.; Zhang, X. Silver-Zwitterion Organic-Inorganic Nanocomposite with Antimicrobial and Antiadhesive Capabilities. *Langmuir* **2013**, *29*, 3773−3779.
(37) Zhang, Q. M.; Serpe, M. J. Synthesis, Characterization, and Antibacterial Properties of a Hydroxyapatite Adhesive Block Copolymer. *Macromolecules* **2014**, *47*, 8018−8025.
(38) Tan, M.; Wang, H.; Wang, Y.; Chen, G.; Yuan, L.; Chen, H. Recyclable Antibacterial Material: Silicon Grafted with 3,6-O-Sulfated Chitosan and Specifically Bound by Lysozyme. *J. Mater. Chem. B* **2014**, *2*, 569−576.
(39) Zhao, C.; Zheng, J. Synthesis and Characterization of Poly(*N*-hydroxyethylacrylamide) for Long-Term Antifouling Ability. *Biomacromolecules* **2011**, *12*, 4071−4079.
(40) Orhan, M.; Kut, D.; Gunesoglu, C. Improving the Antibacterial Activity of Cotton Fabrics Finished with Triclosan by the Use of 1,2,3,4-Butanetetracarboxylic Acid and Citric Acid. *J. Appl. Polym. Sci.* **2009**, *111*, 1344−1352.
(41) Zhang, W.; Chu, P. K.; Ji, J.; Zhang, Y.; Liu, X.; Fu, R. K.; Ha, P. C.; Yan, Q. Plasma Surface Modification of Poly Vinyl Chloride for Improvement of Antibacterial Properties. *Biomaterials* **2006**, *27*, 44−51.
(42) Chen, W.; Liu, Y.; Courtney, H. S.; Bettenga, M.; Agrawal, C. M.; Bumgardner, J. D.; Ong, J. L. In Vitro Anti-Bacterial and Biological Properties of Magnetron Co-Sputtered Silver-Containing Hydroxyapatite Coating. *Biomaterials* **2006**, *27*, 5512−5517.
(43) Wu, H.; Tan, L.; Yang, M.; Liu, C.; Zhuo, R. Protein-Resistance Performance of Amphiphilic Copolymer Brushes Consisting of Fluorinated Polymers and Polyacrylamide Grafted from Silicon Surfaces. *RSC Adv.* **2015**, *5*, 12329−12337.
(44) Narumi, A.; Chen, Y.; Sone, M.; Fuchise, K.; Sakai, R.; Satoh, T.; Duan, Q.; Kawaguchi, S.; Kakuchi, T. Poly(*N*-hydroxyethylacrylamide) Prepared by Atom Transfer Radical Polymerization as a Nonionic, Water-Soluble, and Hydrolysis-Resistant Polymer and/or Segment of Block Copolymer with a Well-Defined Molecular Weight. *Macromol. Chem. Phys.* **2009**, *210*, 349−358.
(45) Zhao, C.; Chen, Q.; Patel, K.; Li, L.; Li, X.; Wang, Q.; Zhang, G.; Zheng, J. Synthesis and Characterization of pH-Sensitive Poly(*N*-2-hydroxyethyl acrylamide)−Acrylic Acid (Poly(HEAA/AA)) Nanogels with Antifouling Protection for Controlled Release. *Soft Matter* **2012**, *8*, 7848−7857.
(46) Apel, C.; Barg, A.; Rheinberg, A.; Conrads, G.; Wagner-Döbler, I. Dental Composite Materials Containing Carolacton Inhibit Biofilm Growth of Streptococcus Mutans. *Dent. Mater.* **2013**, *29*, 1188−1199.
(47) Cringus-Fundeanu, I.; Luijten, J.; van der Mei, H. C.; Busscher, H. J.; Schouten, A. J. Synthesis and Characterization of Surface-Grafted Polyacrylamide Brushes and Their Inhibition of Microbial Adhesion. *Langmuir* **2007**, *23*, 5120−5126.
(48) Costerton, J.; Stewart, P.; Greenberg, P. Bacterial Biofilms: A Common Cause of Persistent Infections. *Sci. Technol. Adv. Mater.* **1999**, *284*, 1321−1318.
(49) Schweizer, H. Triclosan: A Widely Used Biocide and Its Link to Antibiotics. *FEMS Microbiol. Lett.* **2001**, *202*, 1−7.
(50) Braoudaki, M.; Hilton, A. C. Mechanisms of Resistance in *Salmonella enterica* Adapted to Erythromycin, Benzalkonium Chloride and Triclosan. *Int. J. Antimicrob. Agents* **2005**, *25*, 31−37.
(51) Zhao, C.; Li, L.; Zheng, J. Achieving Highly Effective Nonfouling Performance for Surface-Grafted Poly(HPMA) via Atom-Transfer Radical Polymerization. *Langmuir* **2010**, *26*, 17375−17382.
(52) Roosjen, A.; Norde, W.; Mei, H. C.; Busscher, H. J. The Use of Positively Charged or Low Surface Free Energy Coatings versus Polymer Brushes in Controlling Biofilm Formation. *Prog. Colloid Polym. Sci.* **2006**, *132*, 138−144.
(53) Nejadnik, M. R.; van der Mei, H. C.; Norde, W.; Busscher, H. J. Bacterial Adhesion and Growth on a Polymer Brush-Coating. *Biomaterials* **2008**, *29*, 4117−4121.
(54) Saldarriaga Fernandez, I.; Mei, H.; Metzger, S.; Grainger, D.; Engelsman, A.; Nejadnik, M.; Busscher, H. In Vitro and in Vivo Comparisons of Staphylococcal Biofilm Formation on a Cross-Linked Poly(ethylene glycol)-Based Polymer Coating. *Acta Biomater.* **2010**, *6*, 1119−1124.

DOI: 10.1021/acsami.5b01210
ACS Appl. Mater. Interfaces 2015, 7, 7008−7015